Integrated Trajectory and Navigation Design in Unstable Orbital Environments

D. J. Scheeres[1] and M. W. Lo[2]

In the unstable orbital environments about the Earth–Sun and Earth–Moon libration points, the traditional approach of separating trajectory and navigation design can show its limitations. Traditional approaches to navigation design may yield tracking schedule and measurement requirements that are burdensome with no direct indication of how they could be reduced or made more manageable by shifting the nominal trajectory. An integrated approach to trajectory and navigation design would allow a trajectory to be constrained by fundamental navigation metrics in addition to the traditional trajectory constraints of fuel and time. To develop such an approach, we are reexamining and reformulating the navigation problem from a dynamical systems perspective. This article will present the basic rationale for integrated trajectory and navigation design in unstable orbital environments, introduce some basic elements of this approach, and provide simple applications of this approach to a model problem.

I. Introduction

This article addresses the development of an integrated approach to trajectory and navigation design, applicable to missions with unstable orbital environments. Traditional approaches to trajectory and navigation design in orbital environments that are relatively stable allow the design of these two mission elements to be separated. This follows directly from navigation design being derived largely from linearized analysis about a nominal, nonlinear trajectory. By navigation design we mean the choice of orbit-determination measurements and their schedule, and the placement of correction maneuvers along the trajectory.

For missions where the spacecraft travels in a slightly perturbed Keplerian orbit, such as an interplanetary transfer, the design of the navigation system can be easily separated from the design of the trajectory itself, and can be performed after the fact, allowing for an assembly-line style of mission design. In more challenging missions involving gravity assists, such as planetary flybys or satellite orbital tours, the nominal trajectory can no longer be viewed as stable in a traditional sense because orbit-determination errors now get expanded hyperbolically through each planetary or satellite flyby. However, since these flybys occur at well-spaced intervals and the orbit is stable between flybys, the navigation design process can still

[1] Department of Aerospace Engineering, University of Michigan, Ann Arbor.

[2] Navigation and Mission Design Section.

The research described in this publication was carried out by the Jet Propulsion Laboratory, California Institute of Technology, under a contract with the National Aeronautics and Space Administration.

be separate from and follow the trajectory design process. In these situations, the navigation design must concentrate measurements at specific times relative to the flybys in order to ensure that the trajectory uncertainties and their mappings are properly constrained. In these situations, the orbit-determination measurements are chosen, in part, to ensure that the uncertainty mappings never get beyond the linear regime, meaning that the phase volume is never allowed to become significantly stretched in phase space.

When orbital missions are considered in continuously unstable dynamical systems, the situation changes. Examples of such environments would be a Sun–Earth halo orbiter, an Earth–Moon halo orbiter, a Europa Orbiter, or other environments where trajectories are continuously subject to large perturbations that cause neighboring trajectories to diverge from each other hyperbolically over all time spans. A description of orbit determination in these environments is given in [11].

In unstable environments, the traditional approach of separating trajectory and navigation design begins to show its limitations. While the traditional assembly-line approach can still be applied, it can yield tracking schedule and measurement requirements that are artificially large and that give no direct indication of how the navigation requirements could be reduced or made more manageable by shifting the nominal trajectory. An integrated approach to trajectory and navigation design would allow for the nominal trajectory to be constrained by fundamental navigation metrics in addition to the traditional trajectory constraints of fuel and time. The development of such an approach, however, requires that the navigation process be reexamined and reformulated from a dynamical systems perspective, work that is currently in process.

This article first reviews navigation fundamentals with a dynamical systems perspective. Next, for motivation, we introduce some model problems of unstable orbital environments, along with a simple 1-degree-of-freedom (1-DOF) unstable model that can be used to motivate analytical evaluation. Then we develop analysis methods for the navigation of spacecraft in such unstable environments, and apply them to our simple 1-DOF model.

II. Navigation Fundamentals

First we review some fundamental results for spacecraft navigation. We assume a general approach to the problem in what follows, and assume that the dynamical system can be expressed in so-called Hamilton canonical form. That this is possible is trivially true, since the standard Newton's equations of motion in an inertial frame are already in such a form.

A. Dynamical System

Our dynamical state is defined as a six-dimensional vector, $\mathbf{x}$, in general, consisting of three coordinates, $\mathbf{q}$, and three momenta or velocities, $\mathbf{p}$, arranged as $\mathbf{x} = [\mathbf{q}; \mathbf{p}]$. A solution of the dynamical system is designated as $\mathbf{x}(t) = \phi(t, t_o, \mathbf{x}_o, \mu)$, where $\mathbf{x}_o$ is the spacecraft state at an epoch t_o and μ is a vector of force parameters that influence the dynamics of the system. In this article, we do not consider the effect of force parameters on spacecraft navigation, although these are items of essential concern. The state satisfies a differential equation, $\dot{\mathbf{x}}(t) = \mathbf{F}(\mathbf{x}(t), t)$, where the force function, $\mathbf{F}$, is in general a function of both time and the state. Since this is a Hamiltonian system, $\mathbf{F} = J\partial H/\partial \mathbf{x}$, where $H(\mathbf{x}, t)$ is the Hamiltonian of the system. Note that we do not assume that the Hamiltonian is constant in our discussions, thus allowing for a time-varying system. The matrix J is

$$J = \begin{bmatrix} O & I \\ -I & O \end{bmatrix} \tag{1}$$

where O and I are three-by-three zero and identity matrices, respectively.

Associated with each particular flow $\phi(t, t_o, \mathbf{x}_o)$ in phase space is a neighboring flow, corresponding to an initial condition $\mathbf{x}_o + \delta\mathbf{x}$. In general, $\delta\mathbf{x}$ is defined over an arbitrary distribution, but if the size of $\delta\mathbf{x}$ is relatively small, we find that it obeys a linear dynamics law:

$$\delta\dot{\mathbf{x}} = J\frac{\partial^2 H}{\partial \mathbf{x}^2}\delta\mathbf{x} \tag{2}$$

where the matrix $A = J(\partial^2 H/\partial\mathbf{x}^2)$ is evaluated along the nominal solution of the differential equation $\mathbf{x}(t)$. Solving this linear dynamical equation from an initial state, $\mathbf{x}_o$, to a final state, $\mathbf{x}(t)$, results in the general solution:

$$\delta\mathbf{x} = \Phi(t, t_o, \mathbf{x}_o)\delta\mathbf{x}_o \tag{3}$$

where Φ is a six-by-six matrix with unity determinant (due to Liouville's theorem), $\delta\mathbf{x}_o$ is the initial deviation from the state $\mathbf{x}_o$, and $\delta\mathbf{x}$ is the computed linear deviation from the nominal trajectory. While only approximate, this is a powerful result because it provides a general (linear) solution to the dynamical equations in the vicinity of any nominal trajectory.

Corresponding to any region of phase space, $\mathcal{B}_o$, there exists a corresponding region in which the flow of the system is defined, denoted as $\mathcal{B}(t) = \phi(t, t_o, \mathcal{B}_o)$. In particular, if we restrict the size of $\mathcal{B}_o$, we find an explicit solution for $\mathcal{B}(t)$ from the linear dynamics, namely that $\phi(t, t_o, \mathcal{B}_o) = \phi(t, t_o, \mathbf{x}_o)$ $+ \Phi(t, t_o)\delta\mathbf{x}_o; \delta\mathbf{x}_o \in \mathcal{B}_o - \mathbf{x}_o$.

B. State Measurements and Orbit Determination

The second building block of a navigation system, following proper specification of the dynamics, is the specification of the orbit-determination measurements. These generally can be denoted as scalar functions of the state, time, and measurement parameters as $h(\mathbf{x}, t, p)$, where p is the vector of measurement parameters. The quantity h represents some measurable component of the spacecraft state or some combination of these components. Usual quantities are a line-of-sight velocity (Doppler shift), range (light time), or an angle relative to some landmark (optical or very long baseline interferometry (VLBI)-type measurements), where the actual observations are denoted as $\tilde{h}$. For a spacecraft moving along a trajectory, we denote a series of measurements, each taken at a different time t_i, by the sequence $\tilde{h}_i$ and the corresponding functional values for an assumed trajectory $\mathbf{x}(t_i) = \phi(t_i, t_o, \mathbf{x}_o)$ as $h_i = h(\mathbf{x}(t_i), t_i, p)$. We note that the observables $\tilde{h}_i$ are equal to the observable function evaluated at the "true" state $\mathbf{x}^*$, denoted by $h_i^* = h(\mathbf{x}^*, t_i, p)$, plus a measurement noise, ω_i, which is usually assumed to be uncorrelated in time (white) and to follow Gaussian statistics with a zero-mean and a variance, σ_i^2.

Then the orbit-determination problem can be solved by choosing the initial state, $\mathbf{x}_o$, such that the functional $L = \sum_{i=1}^{N} w_i(\tilde{h}_i - h_i)^2$ is minimized, where the w_i are weights that will be defined later. The necessary conditions for the minimum of L to exist are $\partial L/\partial\mathbf{x}_o = 0$, or

$$\sum_{i=1}^{N} w_i \left(\tilde{h}_i - h_i\right) h_{x_i}^T \Phi(t_i, t_o, \mathbf{x}_o) = 0 \tag{4}$$

where $\Phi(t_i, t_o, \mathbf{x}_o) = \partial\mathbf{x}/\partial\mathbf{x}_o|_{t_i}$ and $h_{x_i} = (\partial h/\partial\mathbf{x})|_{t_i}$. These necessary conditions are nonlinear, since the initial state $\mathbf{x}_o$ is present implicitly in h_i, h_{x_i} and in Φ_i.

In practice, one assumes that a nominal trajectory is defined that is relatively close to the true trajectory in phase space, and that a small correction to the initial nominal state can satisfy the necessary

conditions. Specifically, we wish to increment the nominal solution to $\mathbf{x}_o + \delta\mathbf{x}_o$ and solve for the linear correction. Taking the transpose of the above expression, substituting $\mathbf{x}_o + \delta\mathbf{x}_o$ for $\mathbf{x}_o$, and performing the expansion in $\delta\mathbf{x}_o$, we find the new necessary conditions:

$$\sum_{i=1}^{N} w_i \Phi_i^T h_{x_i} z_i - \sum_{i=1}^{N} w_i \Phi_i^T h_{x_i} h_{x_i}^T \Phi_i \delta\mathbf{x}_o + \mathcal{O}\left(\delta\mathbf{x}_o^2\right) = 0 \tag{5}$$

where $z_i = \tilde{h}_i - h_i$ is ideally equal to the data noise if the nominal orbit equals the true orbit; thus, we can never recover the exact conditions due to the noise terms. Ignoring higher-order terms, we can immediately solve for the correction $\delta\mathbf{x}_o$ to satisfy the necessary conditions:

$$\delta\mathbf{x}_o = \Lambda^{-1} \sum_{i=1}^{N} w_i \Phi_i^T h_{x_i} z_i \tag{6}$$

$$\Lambda = \sum_{i=1}^{N} w_i \Phi_i^T h_{x_i} h_{x_i}^T \Phi_i \tag{7}$$

where Λ is referred to as the information matrix at the epoch t_o and will be invertible if the observations taken together span the full initial state. Since this is only an approximate solution, the procedure must be iterated to solve the nonlinear conditions, Eq. (4). In general, if the nominal solution is close enough to the true solution, this iteration procedure will converge on the so-called least-squares orbit-determination solution.

With every measurement or series of measurements, we can assign an information matrix, denoted here as $\delta\Lambda$, which adds to the current information matrix at epoch. From Eq. (7), we see that, in general, $\delta\Lambda = w_i \Phi_i^T h_{x_i} h_{x_i}^T \Phi_i$. Because the measurements will occur at discrete times, we do not consider continuous formulations of measurement updates and instead represent the effect of a measurement at some time t as $\Lambda' = \Lambda + \delta\Lambda$, where Λ' is the new information matrix, all evaluated at epoch. Analogous formulae can be found for the covariance matrix, and, if the measurement is a scalar, a particularly efficient form of an update formula can be found (using the Schuur identity). Computationally, the measurement information updates usually are defined as a Householder transformation operating on a square-root information matrix, as described in [1].

C. Distributions of Orbit Uncertainty

Since the orbit-determination procedure outlined above contains uncertain data measurement terms, which can be described statistically, the resulting solutions for the orbit must also be, in some sense, uncertain and describable using statistical concepts. We formalize these statements in the following.

1. Statistical Description of Orbits. First, under the assumption that the measurement noise has zero mean (which means that there are no unmodeled biases in the measurement function h), is uncorrelated in time, and has a Gaussian distribution at each time step, it can be shown that the true solution equals the mean solution of the distribution. Furthermore, if the data weights are chosen such that $w_i = 1/\sigma_i^2$, then the information matrix Λ is the inverse of the state covariance matrix, P. Finally, it can be shown that the probability density function (pdf) of the initial conditions can be described as

$$f(\mathbf{x}; \overline{\mathbf{x}}, P) = \frac{1}{(2\pi)^{N/2}\sqrt{|P|}} e^{-(1/2)\delta\mathbf{x}\Lambda\delta\mathbf{x}} \tag{8}$$

where $\delta\mathbf{x} = \mathbf{x} - \overline{\mathbf{x}}$ and N is the dimension of $\mathbf{x}$.

Using the pdf, we can define the mean of the solution:

$$\overline{\mathbf{x}} = \int_{\infty} \mathbf{x} f(\mathbf{x}; \overline{\mathbf{x}}, P) d\mathbf{x} \tag{9}$$

the covariance of the solution:

$$P = \int_{\infty} \left[\mathbf{x} - \overline{\mathbf{x}}\right]^T \left[\mathbf{x} - \overline{\mathbf{x}}\right] f(\mathbf{x}; \overline{\mathbf{x}}, P) d\mathbf{x} \tag{10}$$

and the probability that a spacecraft resides in some region $\mathcal{B}$ of phase space:

$$\mathcal{P}(\mathbf{x} \in \mathcal{B}) = \int_{\mathcal{B}} f(\mathbf{x}; \overline{\mathbf{x}}, P) d\mathbf{x} \tag{11}$$

The integral $\int_{\infty}$ is taken over the entire phase space, while the probability integral is taken only over the phase volume contained in the region $\mathcal{B}$.

While the description of the solution mean, covariance, and probability at the initial epoch t_o is useful, we would like to generalize this result to an arbitrary time. The covariance and information matrices both can be viewed as dynamical quantities that vary in time, satisfying the equations

$$\dot{P} = AP + PA^T \tag{12}$$

$$\dot{\Lambda} = -A^T\Lambda - \Lambda A \tag{13}$$

where $A = JH_{\mathbf{xx}}$ has been defined previously. This allows us to specify the covariance and information matrices as functions of time: $\Lambda(t, t_o, \Lambda_o, \mathbf{x}_o)$ and $P(t, t_o, P_o, \mathbf{x}_o)$, where we have noted the explicit dependence of these dynamical quantities on the initial state and initial distributions. The specific solution to these equations can be formulated in terms of the state transition matrix:

$$P(t, t_o) = \Phi(t, t_o) P_o \Phi^T(t, t_o) \tag{14}$$

$$\Lambda(t, t_o) = \Phi^{-T}(t, t_o) \Lambda_o \Phi^{-1}(t, t_o) \tag{15}$$

Thus, the pdf and the probability distribution can be defined as general functions of time:

$$f\left(\mathbf{x}; \overline{\mathbf{x}(t)}, P(t)\right) = \frac{1}{(2\pi)^3 \sqrt{|P(t)|}} e^{-(1/2)\delta\mathbf{x}\Lambda(t)\delta\mathbf{x}} \tag{16}$$

$$\mathcal{P}(\mathbf{x} \in \mathcal{B}) = \int_{\mathcal{B}(t)} f\left(\mathbf{x}; \overline{\mathbf{x}(t)}, P(t)\right) d\mathbf{x} \tag{17}$$

The above equations neglect the effect of model and measurement parameter uncertainties, which can be brought into the dynamical equations for the covariance and information matrices [12].

2. Probability Measure as an Integral Invariant. First, consider some region of phase space, $\mathcal{B}_o$, defined at an initial epoch, t_o. As mentioned above, we can compute the probability that the spacecraft can be found within this phase volume as $\mathcal{P}(\mathbf{x} \in \mathcal{B}_o)$. There are two quantities of interest that can be attached to this idea; the first is the evolution of the phase volume $\mathcal{B}_o$ as a function of time, and the second is the probability that the spacecraft will remain within this volume as time progresses. The first consideration can be understood, in a nonstatistical sense, as the evolution of the phase volume:

$$V(t) = \int_{\mathcal{B}(t)} d\mathbf{x} = \int_{\phi(t,t_o,\mathcal{B}_o)} d\mathbf{x} \tag{18}$$

where the integral occurs over the six-dimensional region $\mathcal{B}(t)$ mapped in time. Since we have assumed a Hamiltonian structure to our dynamics, we can immediately apply Liouville's theorem [6] and note that the volume is conserved. This is an instance of an absolute integral invariant, stating that an integrated quantity defined over an arbitrary region of phase space is constant in time. Formally, a phase-space integral of maximal order can be stated as

$$I = \int_{\mathcal{B}} M(\mathbf{x}, t) d\mathbf{x} \tag{19}$$

where we assume that the state follows the dynamics equation $\dot{\mathbf{x}} = \mathbf{F}(\mathbf{x}, t)$. A necessary condition for I to be an integral invariant is that the scalar quantity M satisfies the condition [6]

$$\frac{dM}{dt} + M \text{trace}\left(\frac{\partial \mathbf{F}}{\partial \mathbf{x}}\right) = 0 \tag{20}$$

For the case where $M = 1$, we see that $I = V$, the phase volume. In this case, $dM/dt = 0$, and the condition reduces to trace $(\partial \mathbf{F}/\partial \mathbf{x}) = 0$. Now recall that we are dealing with Hamiltonian dynamical systems, so $\mathbf{F} = J\partial H/\partial \mathbf{x}$. Allowing the state $\mathbf{x}$ to be split into vectors of coordinates, $\mathbf{q}$, and momenta, $\mathbf{p}$, we have $\mathbf{x} = [\mathbf{q}, \mathbf{p}]$, and we find the general result that $\dot{q}_i = \partial H/\partial p_i$ and $\dot{p}_i = -\partial H/\partial q_i$. This leads to

$$\text{Trace}\left(J\frac{\partial^2 H}{\partial \mathbf{x}^2}\right) = \sum_{i=1}^{n}\left[\frac{\partial^2 H}{\partial q_i \partial p_i} - \frac{\partial^2 H}{\partial p_i \partial q_i}\right] = 0 \tag{21}$$

establishing Liouville's theorem.

It should be noted that the application given above assumes that the force parameters of the system are fixed and have no range of uncertainties associated with them. This is a reasonable restriction on the system, but one that cannot always be applied when we speak of statistical distributions.

Now note that the probability measure defined previously in Eq. (11) is in the proper form to be an integral invariant. Thus, we can check to see if the probability measure is invariant under the dynamics of the system, where the pdf function f is identified with the M function in Eq. (19). In the following, we will assume that the region over which we integrate to find the probability of our system is relatively small compared to the actual state components, allowing us to use the linearized flow to describe motion. Let us restate the pdf, now set equal to the M functional, as

$$M(\mathbf{x}, t) = \frac{1}{(2\pi)^3}|\Lambda(t)|^{1/2} e^{-(1/2)\delta\mathbf{x}^T \Lambda(t)\delta\mathbf{x}} \tag{22}$$

where $\delta\mathbf{x} = \mathbf{x} - \mathbf{x}_M$ and $\mathbf{x}_M$ is the mean of the distribution. Assume that force model uncertainties are not included in the information matrix (although measurement parameter uncertainties can be included without affecting the following). From the above, we already see that the second factor in Condition (20) is satisfied, as we assume a Hamiltonian dynamical system. Thus, we only need to establish that $dM/dt = 0$, or

$$\frac{1}{(2\pi)^3}|\Lambda(t)|^{1/2}e^{-(1/2)\delta\mathbf{x}^T\Lambda(t)\delta\mathbf{x}}\left\{\frac{|\dot{\mathbf{\Lambda}}|}{|\mathbf{\Lambda}|} - \frac{1}{2}\left[\delta\dot{\mathbf{x}}^T\Lambda\delta\mathbf{x} + \dot{\mathbf{x}}^T\Lambda\delta\dot{\mathbf{x}} + \dot{\mathbf{x}}^T\dot{\Lambda}\delta\mathbf{x}\right]\right\} = 0 \tag{23}$$

First consider the time derivative of $|\Lambda|$. It can be shown that [6]

$$\frac{d|\Lambda|}{dt} = -2|\Lambda|\text{Trace}(A) \tag{24}$$

$$\text{trace}(A) = \sum_{i=1}^{n}\left[\frac{\partial^2 H}{\partial q_i \partial p_i} - \frac{\partial^2 H}{\partial p_i \partial q_i}\right] \tag{25}$$

which was the same condition as for Liouville's theorem, and thus the determinant of Λ (and also P) is a constant. It is important to note that this is no longer true if force model parameter uncertainties are included, as then the information content will have a uniform decrease in time. Next consider the time derivative of the exponential function. Now we will invoke a linearization assumption to assume that $\delta\dot{\mathbf{x}} = A\delta\mathbf{x}$. The condition then becomes

$$\delta\mathbf{x}^T\left[A^T\Lambda + \Lambda A + \dot{\Lambda}\right]\delta\mathbf{x} = 0 \tag{26}$$

which is trivially satisfied, given Eq. (13), if no uncertainty in the force parameters is assumed. Thus, we see that the probability of finding a spacecraft within a given region is an integral invariant if there are no uncertainties in the force model, meaning that this probability does not change its value over time.

This may seem like an obvious result, but we note that, if force parameter uncertainties are included into the dynamics of Λ, this is no longer true and that the probability of finding a spacecraft within one evolving region of phase fluid is not constant in time. What occurs in this case is that the uncertainties in the dynamics allow possible trajectories to leave the nominally defined phase fluid volume. An interesting question is whether a suitably generalized description of the dynamics would allow the integral invariance to hold again. A deeper understanding of what occurs in these cases is still needed. In the following, we will ignore the case of uncertain force parameters, focusing instead on the simpler case.

3. Probability Computation. As discussed above, the region over which we compute the probability of finding a spacecraft is arbitrary. However, in practice it is common to restrict this region to a generalized ellipsoid that uses the information matrix as a generator. The reasons for this restriction are twofold. First, it turns out that the probability computation over this region can be evaluated in closed form and is directly related to χ^2-probability distributions. Second, the probability ellipsoids are themselves invariants of the flow and map into each other. Should we consider some other region of phase space over which the probability computation would be carried out, we would not have these two properties, even though the probability measure would still be constant.

Specifically, let us consider the probability of finding the spacecraft within a region defined by the ellipsoid:

$$\delta\mathbf{x}^T\Lambda\delta\mathbf{x} \leq r^2 \tag{27}$$

where r is an arbitrary number, and $\delta\mathbf{x}$ and Λ can be considered to be evaluated at epoch. Then, $\mathcal{B} = \left\{\delta\mathbf{x} \mid r^2 - \delta\mathbf{x}^T\Lambda\delta\mathbf{x} \geq 0\right\}$. Thus, the probability integral can be stated as

$$\mathcal{P}(\delta\mathbf{x} \in \mathcal{B}) = \frac{1}{(2\pi)^{N/2}\sqrt{|P|}} \int_{\mathcal{B}} e^{-(1/2)\mathbf{x}^T\Lambda\mathbf{x}} d\mathbf{x} \tag{28}$$

By suitable change of variables, this can be reduced to the form (for general N)

$$\mathcal{P} = \frac{2}{2^{N/2}\Gamma(N/2)} \int_0^r u^{N-1} e^{-(1/2)u^2} du \tag{29}$$

where $\Gamma(n) = (n-1)!$ and $\Gamma(n+1/2) = \sqrt{\pi}(2n)!/2^{2n}/n!$, where n is an integer. The coefficient represents the integral over the surface of a sphere in N dimensions divided by $(2\pi)^{N/2}$, and the remaining integral represents the integral over the radius of that sphere. For the general case of spacecraft motion, $N = 6$ and the coefficient of the integral is $1/8$. This integral can be rewritten in a standard form:

$$\mathcal{P} = \frac{1}{2^{N/2}\Gamma(N/2)} \int_0^{r^2} x^{[(N-2)/2]} e^{-(1/2)x} dx \tag{30}$$

which is in the classic χ^2-probability integral form, for which tables exist.

In usual navigation practice, the state of the spacecraft is desired only on some lower-dimensional surface. A classic example is the computation of probability of the spacecraft when projected onto the plane perpendicular to the approach trajectory to a target planet. This represents a computation of probability on a two-dimensional surface, involving only the position components. Further simplifications occur if we map into a one-dimensional subspace, which will happen when we consider the statistics of ΔV consumption to control an orbit. When computing the probability distribution in these subspaces, it is necessary first to compute the relevant pdf for that projection, meaning that the mean and covariance of the new variables must be calculated. Two situations will occur for this case, in general. The first is that the projection is a simple linear combination of the state and can be represented as $\mathbf{q} = \Psi\mathbf{x}$; the second is that the projection is the norm of a linear combination and can be represented as $q = \|\Psi\mathbf{x}\|_2$, the 2-norm of a vector. In both cases, the matrix Ψ is of order $m \times n$, $m \leq n$.

For the first case, we find that the new mean and covariance are simply related to the mean and covariance of the state $\mathbf{x}$:

$$\overline{\mathbf{q}} = \Psi\overline{\mathbf{x}} \tag{31}$$

$$P_{\mathbf{qq}} = \Psi P \Psi^T \tag{32}$$

where $\overline{\mathbf{x}}$ and P are the mean and covariance of the original state $\mathbf{x}$. Then the computation of the probability can proceed using the pdf:

$$f(\mathbf{q}, \overline{\mathbf{q}}, P_{\mathbf{qq}}) = \frac{1}{(2\pi)^{m/2}\sqrt{|P_{\mathbf{qq}}|}} e^{-(1/2)(\mathbf{q}-\overline{\mathbf{q}})^T P_{\mathbf{qq}}^{-1}(\mathbf{q}-\overline{\mathbf{q}})} \tag{33}$$

where we note that the covariance matrix $P_{\mathbf{qq}}$ will be nonsingular in general as $m \leq n$ and P is nonsingular.

For the second case, we see that the computations are simplified in that we must compute only the mean and variance of a scalar, but that the integrations we must perform become more complicated as they are nonlinear in the state $\mathbf{x}$. Specifically, we find

$$\overline{q} = \int_{\infty} \|\Psi \mathbf{x}\|_2 f(\mathbf{x}) d\mathbf{x} \tag{34}$$

$$\sigma_q^2 = \int_{\infty} \left[\|\Psi \mathbf{x}\|_2 - \overline{q}\right]^2 f(\mathbf{x}) d\mathbf{x} \tag{35}$$

The computation for the mean can be bounded. To result in an integrable expression, we must note that the information matrix in the pdf, Λ, can be split arbitrarily into the product of the square-root information matrix $\Lambda = R^T R$ [1]. This is the transformation used to reduce the probability integral to the form found in Eq. (29). Then the change of variables to the vector $\mathbf{u} = R\mathbf{x}$ is performed, where the Jacobian $|\partial x/\partial u| = 1/|R| = \sqrt{|P|}$, resulting in the elimination of the covariance determinant from the integral. Thus, anticipating this transformation, we can rewrite $q = \|\Psi R^{-1}\mathbf{u}\|_2 \leq \|\Psi R^{-1}\|_2 \|\mathbf{u}\|_2$, yielding

$$\overline{q} \leq \|\Psi R^{-1}\|_2 \int_{\infty} \|\mathbf{u}\|_2 f(\mathbf{x}) d\mathbf{x} \tag{36}$$

$$\int_{\infty} \|\mathbf{u}\|_2 f(\mathbf{x}) d\mathbf{x} = \frac{2}{2^{N/2}\Gamma(N/2)} \int_0^{\infty} u^N e^{-(1/2)u^2} du \tag{37}$$

$$= \sqrt{2}\, \frac{\Gamma\left(\frac{N}{2} + \frac{1}{2}\right)}{\Gamma\left(\frac{N}{2}\right)} \tag{38}$$

yielding the inequality

$$\overline{q} \leq \|\Psi R^{-1}\|_2 \sqrt{2}\, \frac{\Gamma\left(\frac{N}{2} + \frac{1}{2}\right)}{\Gamma\left(\frac{N}{2}\right)} \tag{39}$$

A similar bound can't be derived for the variance, due to the subtraction that exists; still, this simplified formula allows for an estimate of the mean without carrying out a detailed integration.

4. Invariance of Geometric Shapes in Linearized Flow. In addition to the integral invariance of volume and probability, certain geometric forms are conserved under the linearized flow of a Hamiltonian dynamical system. It is appropriate to restrict ourselves to linearized flow here, as spacecraft navigation is generally designed to ensure that the statistically significant deviations of a spacecraft lie relatively close to the nominal. Under this constraint, we establish the invariance of some important geometric shapes and surfaces in phase space: a special class of ellipsoids, a general parallelepiped, and a special class of right parallelepipeds.

Invariance of probability ellipsoids. We have already established the invariance of a particular class of ellipsoids, those generated by the information matrix. We designate these sets as $\left\{\mathcal{E} = \delta\mathbf{x}; \delta\mathbf{x}^T \Lambda \delta\mathbf{x} \leq r^2\right\}$, where r is a constant (we will assume $r = 1$ in general). As shown above, these ellipsoids are constant under the dynamics of the flow, since $\dot{\mathcal{E}} = 0$, but their shape and orientation will change along with the information matrix (barring any measurements or force uncertainties). There is also a familiar result in orbit-determination theory that complements this observation, which is that the probability integral can be evaluated easily if one assumes that the domain $\mathcal{B}$ is an ellipsoid in phase space, defined as $\mathcal{E}$. In fact, given such a domain in phase space, the future distributions also will lie within the same general ellipsoidal domain.

Since the ellipsoid $\mathcal{E}$ is determined at each point of time, so are its major axes and their directions, $a_i(t), \mathbf{v}_i(t)$, where the a_i are the semimajor axis lengths and the $\mathbf{v}_i(t)$ are the directions of these axes, with $\mathbf{v}_i \cdot \mathbf{v}_j = \delta_{ij}$. These dimensions and directions are defined at each moment, but do not map into themselves and are instead continuously displaced on the surface of the ellipsoid. Finally, the constant volume of the general ellipsoid is proportional to the product of the a_i; thus, $\Pi_{i=1}^{2n} a_i(t)$ is a constant in time.

Invariance of parallelepipeds. There is no particular reason to choose the domain $\mathcal{B}$ in the probability integral Eq. (11) to be an ellipsoid, other than computational convenience. Thus, if we choose $\mathcal{B}$ to define a parallelepiped instead, the probability measure would still be conserved, although the geometric form of the volume is not as immediately evident. To analyze this, consider the evolution of a parallelepiped under the linearized flow. We mathematically define a parallelepiped for an N-dimensional phase space by considering a set of nonsingular vectors $\mathbf{u}_i; i = 1, 2, \cdots, N$, each with a defined length,u_i, and assume that they form the "corner" of a parallelepiped. Then the corresponding "edge" of a parallelepiped can be generated by the vector $\{\tau\mathbf{u}_i; \tau \in [-1, 1]\}$, and a surface planar area can be generated by the set $\{\tau_i\mathbf{u}_i + \tau_j\mathbf{u}_j; \tau_i \in [-1, 1], \tau_j \in [-1, 1]\}$, which can be generalized to dimension N, yielding the general parallelepiped region: $\{B = \sum \tau_i\mathbf{u}_i; \tau_j \in [-1, 1], j = 1, 2, \cdots, N\}$.

Then, a vector $\delta\mathbf{x} \in B$ if it equals the summation for some set of values of τ. Or, conversely, $\delta\mathbf{x} \in B$ if $[\tau_i] = [\mathbf{u}_i]^{-1}\delta\mathbf{x}$ and $\tau_i \in [-1, 1], i = 1, 2, \cdots, N$. We note that the τ_i serve the role of coordinates in the basis defined by the $\mathbf{u}_i$. The volume of this region is easily computed as $V_B = |2\mathbf{u}_j| = 2^{2n}|\mathbf{u}_j|$, where $|\mathbf{u}_j|$ denotes the determinant of the set of vectors. From Liouville's theorem and the integral invariance of probability distributions, we know that the volume of this set is conserved and that the probability that this volume defines is also conserved.

Now consider the geometry of this shape under linearized flow. Note that an arbitrary point $\delta\mathbf{x}$ will map, relative to the nominal orbit, as $\Phi\delta\mathbf{x}$. Thus, if $\delta\mathbf{x} = \sum \tau_i\mathbf{u}_i$, then $\Phi\delta\mathbf{x} = \Phi\sum \tau_i\mathbf{u}_i = \sum \tau_i\Phi\mathbf{u}_i = \Phi[\mathbf{u}_i][\tau_i]$. Solving for the coordinates τ_i, we find

$$[\tau_i] = [\mathbf{u}_i]^{-1}\Phi^{-1}\Phi\delta\mathbf{x} \tag{40}$$

$$= [\mathbf{u}_i]^{-1}\delta\mathbf{x} \tag{41}$$

Thus, we see that the new, mapped point can be expressed with the same coordinates τ_i, and thus will remain within the defined parallelepiped. We should note that the volume of this new shape is $V_B = 2^{2n}|\Phi||\mathbf{u}_j|$, and that $|\Phi| = 1$, showing volume conservation. While the volume is conserved, the relative orientation of the vectors and their lengths are not conserved. This situation has been studied previously in the context of Lyapunov characteristic exponents [4]. In an unstable trajectory, we would expect the parallelepiped to become stretched along the unstable directions and compressed along the stable directions, while keeping its basic parallelepiped shape. Finally, it should be noted that, since the coordinates τ_i are conserved under the linear flow, a surface segment of the parallelepiped, defined by one or more coordinates being at an extreme value of ± 1, will be mapped into itself.

Invariance of a class of right parallelepipeds. Finally, we note the invariance of a class of right parallelepipeds, i.e., parallelepipeds where all the $\mathbf{u}_i$ are orthogonal to each other, related to the probability ellipsoids. We know from above that such a shape will not conserve orthogonality under the linearized flow. However, due to the existence of the invariant probability ellipsoids, we can establish the existence of a class of right parallelepipeds that always exist and contain some invariance properties, even though they are not directly invariant under the flow.

Define the right parallelepipeds $R = \sum_{i=1}^{2n} \tau_i a_i \mathbf{v}_i; \tau_j \in [-1, 1], j = 1, 2, \cdots, 2n$, where the a_i and $\mathbf{v}_i$ are defined above as the square root of the eigenvalues of the covariance matrix and their corresponding eigenvectors. These shapes do not map into themselves under the dynamical flow, but are well defined at each instant of time. Furthermore, they have a constant volume because the volume of the parallelepiped in this case is $2^{2n}\Pi_{i=1}^{2n} a_i$, which is proportional to the ellipsoid volume, a constant. However, the probability of finding the spacecraft within this special class of volumes is not necessarily conserved since the shape does not map into itself under the Hamilton flow, which is required for the integral invariance result stated earlier to hold. It would be interesting to investigate this point further, to definitely show whether or not this supposition is true.

D. Statistical Maneuver Design

To plan for the navigation of a spacecraft, it is necessary to develop a statistical model for the amount of fuel that will be necessary to keep the spacecraft on course. With the above results and definitions, such an analysis can be performed. In its most general form, the problem can be stated as follows. Given an error in position and velocity relative to the nominal trajectory at time t_o of the form $\delta\mathbf{r}_o$, $\delta\mathbf{v}_o$, what is the mean and variance in the cost of the maneuvers to reduce the system back to $\delta\mathbf{r} = \delta\mathbf{v} = 0$ at some future time? Generally, the errors in position and velocity arise from the previous maneuver and can be thought of as errors in knowledge of the spacecraft state. Practically, maneuver execution errors also must be incorporated, but let us ignore these for the moment.

For a general trajectory, a minimum of two maneuvers are required to get back on track: one maneuver to target back to the trajectory at some future time and a second maneuver to reduce the relative velocity to zero at that crossing. Of course, at the time when the trajectory crossing occurs, errors from the epoch of the last maneuver manifest themselves in a new set of dispersions, which must themselves be corrected. By considering the new dispersions to be uncorrelated with the initial dispersions (a conservative assumption in general), we can isolate these effects from each other and perform an analysis on the two maneuvers alone. For the design of these maneuvers, we have two free parameters, the time from the initial epoch at which we perform the first correction maneuver, t_1, and the time at which the trajectory crossing will occur, t_2. In some instances, it is possible to choose $t_2 - t_1 \gg t_1 - t_o$. Then the correction maneuvers will occur after a time interval of $t_1 - t_o$, and essentially the second maneuvers will never occur, as each correction maneuver will retarget the second maneuver based on new measurements.

We can express the maneuver strategy explicitly. Assume the state transition matrix is partitioned as

$$\Phi(t, t_o) = \begin{bmatrix} \phi_{rr} & \phi_{rv} \\ \phi_{vr} & \phi_{vv} \end{bmatrix} \tag{42}$$

Then, given a set of initial errors at epoch t_o, $\delta\mathbf{r}_o$ and $\delta\mathbf{v}_o$, the state of the system at a later time t_1 is

$$\delta\mathbf{r}_1 = \phi_{rr}(t_1, t_o)\delta\mathbf{r}_o + \phi_{rv}(t_1, t_o)\delta\mathbf{v}_o \tag{43}$$

$$\delta\mathbf{v}_1 = \phi_{vr}(t_1, t_o)\delta\mathbf{r}_o + \phi_{vv}(t_1, t_o)\delta\mathbf{v}_o \tag{44}$$

A targeting maneuver is designed to null the spacecraft position error at some future time t_2, essentially targeting the spacecraft to cross the nominal trajectory:

$$\delta\mathbf{r}_2 = 0 = \phi_{rr}(t_2,t_1)\delta\mathbf{r}_1 + \phi_{rv}(t_2,t_1)\delta\mathbf{v}_1' \tag{45}$$

The first maneuver is then computed as $\Delta V_1 = \delta\mathbf{v}_1' - \delta\mathbf{v}_1$ and is explicitly equal to

$$\begin{aligned}\Delta V_1 = & -\left[\phi_{rv}^{-1}(t_2,t_1)\phi_{rr}(t_2,t_1)\phi_{rr}(t_1,t_o) + \phi_{vr}(t_1,t_o)\right]\delta\mathbf{r}_o \\ & -\left[\phi_{rv}^{-1}(t_2,t_1)\phi_{rr}(t_2,t_1)\phi_{rv}(t_1,t_o) + \phi_{vv}(t_1,t_o)\right]\delta\mathbf{v}_o\end{aligned} \tag{46}$$

The second maneuver is then performed at time t_2 and nulls the relative speed of the spacecraft to the nominal trajectory, $\Delta V_2 = -\delta\mathbf{v}(t_2)$, explicitly leading to

$$\begin{aligned}\Delta V_2 = & \left[\phi_{vv}(t_2,t_1)\phi_{rv}^{-1}(t_2,t_1)\phi_{rr}(t_2,t_1)\phi_{rr}(t_1,t_o) - \phi_{vr}(t_2,t_1)\phi_{rr}(t_1,t_o)\right]\delta\mathbf{r}_o \\ & + \left[\phi_{vv}(t_2,t_1)\phi_{rv}^{-1}(t_2,t_1)\phi_{rr}(t_2,t_1)\phi_{rv}(t_1,t_o) - \phi_{vr}(t_2,t_1)\phi_{rv}(t_1,t_o)\right]\delta\mathbf{v}_o\end{aligned} \tag{47}$$

Thus, the general correction maneuver is a formula of the form

$$\Delta V_i = |\Psi_i\delta\mathbf{x}| \tag{48}$$

where Ψ_i is a matrix in general. To compute the statistical cost of these maneuvers requires us to compute the mean and variance:

$$\overline{\Delta V} = \int_\infty \Delta V f(\mathbf{x}_o)d\mathbf{x}_o \tag{49}$$

$$\sigma_{\Delta V}^2 = \int_\infty \left(\Delta V - \overline{\Delta V}\right)^2 f(\mathbf{x}_o)d\mathbf{x}_o \tag{50}$$

$$= \overline{(\Delta V)^2} - \overline{\Delta V}^2 \tag{51}$$

If we implement a series of M such maneuvers, each with the same assumed statistical and dynamical representation, the total mean maneuver cost is $M\overline{\Delta V}$ and the total variance is $M\sigma_{\Delta V}^2$. Thus, if we wish to estimate the statistical cost of performing this sequence of maneuvers to within an n-sigma probability value (1-D Gaussian), we find

$$\Delta V_{stat} = M\left[\overline{\Delta V} + \frac{n}{\sqrt{M}}\sigma_{\Delta V}\right] \tag{52}$$

Instead, if we wish to bound the mean ΔV, we find

$$\overline{\Delta V} \leq \sqrt{2}\,\frac{\Gamma\left(\frac{N}{2}+\frac{1}{2}\right)}{\Gamma\left(\frac{N}{2}\right)}\|\Psi R^{-1}\|_2 \tag{53}$$

where N is the dimension of the phase space being considered and R is the square-root information matrix.

III. Model Problems of Unstable Orbital Environments

Having reviewed the basics of spacecraft navigation, we are interested in developing appropriate performance measures that make sense in unstable orbital environments. Thus, to motivate our discussion, we present some of the model unstable orbital environments that occur for spacecraft in the vicinity of the Earth.

A. General Models in the Earth–Moon–Sun System

For our generic model problem, we take the following general equations of motion:

$$\ddot{x} - 2\dot{y} = \frac{\partial V}{\partial x} \tag{54}$$

$$\ddot{y} + 2\dot{x} = \frac{\partial V}{\partial y} \tag{55}$$

$$\ddot{z} = \frac{\partial V}{\partial z} \tag{56}$$

We consider two generic force functions, the restricted three-body problem and the Hill problem:

$$V_R = \frac{1}{2}\left(x^2+y^2\right) + \frac{1-\mu}{\sqrt{(x-1+\mu)^2+y^2+z^2}} + \frac{\mu}{\sqrt{(x-\mu)^2+y^2+z^2}} \tag{57}$$

$$V_H = \frac{1}{\sqrt{x^2+y^2+z^2}} + \frac{1}{2}\left(3x^2-z^2\right) \tag{58}$$

The restricted three-body problem can be considered as the simplest model of spacecraft motion in the Earth–Moon system and contains a host of interesting unstable motions that spacecraft could be flown in. Recent interest has focused on maintaining halo orbits, or lissajous orbits, in the vicinity of the L_1 libration point (between the Earth and the Moon) as a way station for transfers into the solar system and into the Earth–Sun halo orbits. This is enabled by an historical accident: the current energy levels of the Earth L_1 and L_2 Lagrange points differ from that of the Earth–Moon by only about 50 m/s (as measured by maneuver velocity). The significance of this coincidence to the development of space cannot be overstated. For example, this implies that lunar L_1 halo orbits are connected to halo orbits around Earth's L_1 or L_2 via low energy pathways. Many of NASA's future space observatories located around the Earth's L_1 or L_2 may be built in a lunar L_1 orbit and conveyed to the final destination with minimal propulsion requirements. Similarly, when the spacecraft or instruments require servicing, they may be returned from Earth libration orbits to the lunar L_1 orbit, where human servicing may be performed. Since the lunar L_1 orbit may be reached from Earth in less than a week, the infrastructure and complexity

of long-term space travel is greatly mitigated. The same orbit could reach any point on the surface of the Moon within hours; thus, this portal is also a perfect location for the return of human presence on the Moon. The lunar L_1 orbit is also an excellent point of departure for interplanetary flight, where several lunar and Earth encounters may be added to further reduce the launch cost and open up the launch period. The lunar L_1 is a versatile hub for a space transportation system. Figure 1 shows two halo orbits at the lunar L_1 and L_2, respectively, and the set of invariant manifolds forming the InterPlanetary Superhighway (IPS) that provides low-energy departures from the lunar L_1 orbit. One challenge to the use of these orbits is that motion in the vicinity of the Earth–Moon libration points is dominated by a hyperbolic instability with characteristic time on the order of 2 days. Thus, we expect dynamical instabilities to play an important role in controlling the implementation of spacecraft navigation for such systems.

The Hill restricted three-body problem can be considered to be the simplest model of motion in the Earth–Sun system, and it contains dynamics analogous to the restricted three-body problem in the vicinity of the secondary. The characteristic instability of halo orbits in this problem is on the order of 25 days, much slower than for the Earth–Moon system, but still significant. While there have been several missions to these orbits, it is still considered to be a challenging environment for trajectory design and navigation. This problem has been used recently to develop a basic theory for orbit determination of spacecraft in unstable trajectories [11].

B. Simplified Model for Analytical Study

In this article, we will consider a simplified model for illustrative purposes. This is the 1-degree-of-freedom, unstable dynamical system:

$$\ddot{r} - \lambda^2 r = 0 \tag{59}$$

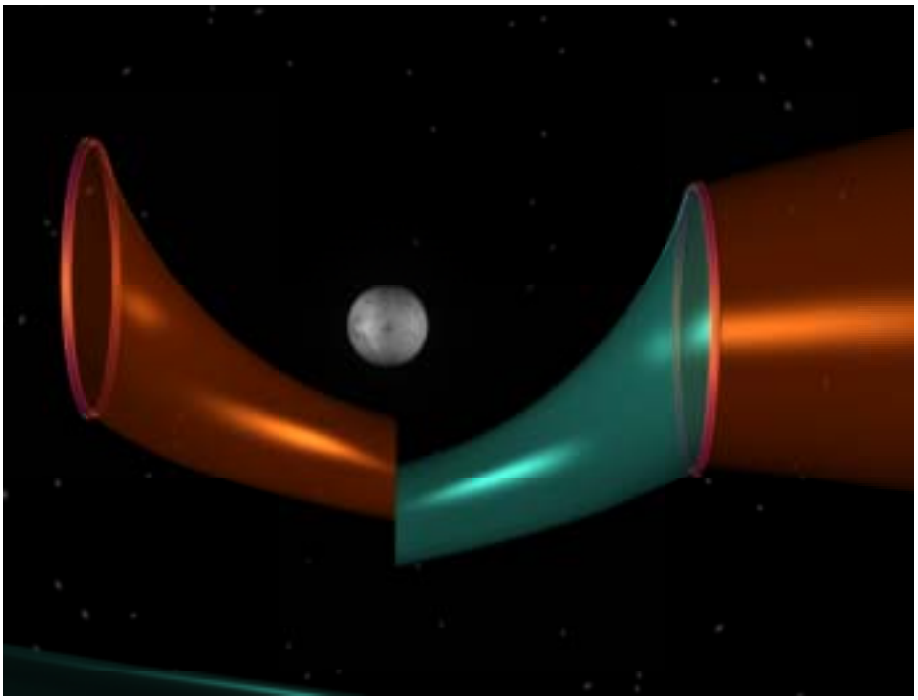

Fig. 1. Two halo orbits at the lunar L_1 and L_2, respectively, and the set of invariant manifolds forming the InterPlanetary Superhighway that provides low-energy departures from the lunar L_1 orbit.

which has a general solution of the form

$$\begin{bmatrix} r(t) \\ v(t) \end{bmatrix} = \Phi(t - t_o) \begin{bmatrix} r(t_o) \\ v(t_o) \end{bmatrix} \tag{60}$$

$$\Phi(t) = \begin{bmatrix} \cosh(\lambda t) & \frac{1}{\lambda}\sinh(\lambda t) \\ \lambda \sinh(\lambda t) & \cosh(\lambda t) \end{bmatrix} \tag{61}$$

Although too simple for direct modeling of a dynamical system, this model contains essential elements of the more complicated unstable systems. Just like the generic instabilities found in the above examples, this model has a single pair of hyperbolic roots, leading to an asymptotically stable and unstable manifold in phase space. At the simplest order, this matches with the unstable dynamical phenomenon found for motion about libration points or in halo orbits. Drawbacks of this model are that the stable and unstable manifolds of the origin coincide in position space, a situation that does not occur for more general models of spacecraft motion, and that there is no central manifold to contend with. Still, the fact that it provides us with an instability of the proper phase-space dimension implies that it can be used as a guide for our thinking.

For this simple system, we note that the characteristic exponent λ defines the direction of the stable and unstable manifolds in phase space, namely that $\lambda = \tan\gamma_m$, where $\pm\gamma_m$ is the direction of the unstable and stable manifolds in (r, v) phase space, respectively. Thus, all motion forward in time will tend towards the direction $n\pi + \gamma_m$, while all motion backwards in time will tend towards the direction $n\pi - \gamma_m$.

IV. Analyzing Navigation in Unstable Environments

Now we wish to derive possible metrics for use in evaluating and modifying the orbit uncertainty, measurement strategy, and maneuver placement. In developing each of these ideas, we will use our simple 1-DOF model to motivate our discussion and indicate possible approaches to the generalized computation of these metrics.

A. Characterizations of Orbit-Uncertainty Distributions

We first consider the geometry of an unstable orbit distribution. We are specifically interested in the direction and extent of the maximum uncertainty of our distribution and convenient ways in which to summarize the global constraints on the uncertainty. We shall see, later, that these play a role in our analysis.

1. Orientation of Distributions. First, consider the computation of the maximum extension that a linear deviation from a trajectory can have, given a constrained initial state. Specifically, we wish to maximize the 2-norm of $\delta\mathbf{x}$ or, equivalently, the function $\delta\mathbf{x}^T\delta\mathbf{x}$ subject to the constraint $\delta\mathbf{x}_o^T\Lambda_o\delta\mathbf{x}_o - 1 = 0$, i.e., the initial distribution lies on an ellipsoid of constant probability. In other words, given an initial probability distribution, what is the maximum state that can result in the future, and what initial conditions lead to this maximum state? To answer this question, we form the augmented Lagrangian:

$$L = \delta\mathbf{x}^T\delta\mathbf{x} - \sigma^2\left(\delta\mathbf{x}_o^T\Lambda_o\delta\mathbf{x}_o - 1\right) \tag{62}$$

$$\delta\mathbf{x} = \Phi(t, t_o)\delta\mathbf{x}_o \tag{63}$$

where σ^2 is the Lagrange multiplier, and compute the extremal conditions $\partial L/\partial\mathbf{x}_o = 0$, leading to

$$\left(\Phi^T\Phi - \sigma^2\Lambda_o\right)\delta\mathbf{x}_o = 0 \tag{64}$$

From this we see that the maximal value of all trajectories given the initial constraint is

$$\delta\mathbf{x}^T\delta\mathbf{x} = \sigma^2 \tag{65}$$

where σ^2 is the maximum eigenvalue of Eq. (64). Thus, the maximum extent that a linear trajectory can have, starting from a constrained state distribution, is the square root of the eigenvalue of $\Lambda_o^{-1}\Phi^T\Phi$. We note that the eigenvector $\delta\mathbf{x}_o$ is not an eigenvector of the matrix Φ in general, and that the resulting direction $\delta\mathbf{x} = \Phi\delta\mathbf{x}_o$ is not necessarily related to the eigenvectors of Φ either. For time-invariant systems, or for time-periodic systems, these two can approach each other when the time grows arbitrarily long. For generalized motion, however, there is not necessarily a relationship between these quantities.

Next, let us consider the direction of maximum uncertainty of a trajectory evaluated at a given time. We restrict ourselves to trajectory dispersion distributions that initially lie within an ellipsoidal region, and hence will always remain within an ellipsoidal region: $\delta\mathbf{x}^T\Lambda(t,t_o)\delta\mathbf{x} \leq 1$. Now we recall that the information matrix can be mapped in time using the state transition matrix (in the absence of stochastic acceleration noise) $\Lambda(t,t_o) = \Phi(t,t_o)^{-T}\Lambda_o\Phi(t,t_o)^{-1}$, and we wish to maximize the value of $\delta\mathbf{x}(t)^T\delta\mathbf{x}(t)$ subject to lying on the surface of the probability ellipsoid, leading to the Lagrangian:

$$L = \delta\mathbf{x}^T\delta\mathbf{x} - \sigma^2\left(\delta\mathbf{x}^T\Lambda(t,t_o)\delta\mathbf{x} - 1\right) \tag{66}$$

and the extremal condition $\partial L/\partial\delta\mathbf{x} = 0$:

$$\left[\frac{1}{\sigma^2}I - \Lambda(t,t_o)\right]\delta\mathbf{x} = 0 \tag{67}$$

Again, the maximal value of all trajectories given the final constraint is

$$\delta\mathbf{x}^T\delta\mathbf{x} = \sigma^2 \tag{68}$$

where $1/\sigma^2$ is the minimum eigenvalue of the information matrix $\Lambda(t)$. Now note that the problem can be transformed by multiplying by the covariance matrix $P(t,t_o) = \Lambda(t,t_o)^{-1}$ to find

$$\left[P(t,t_o) - \sigma^2 I\right]\delta\mathbf{x} = 0 \tag{69}$$

showing the equivalence of evaluating the distribution in terms of covariance or in terms of the information matrix.

Now, to close the circle, let us evaluate the trajectory along the initial condition in Eq. (64) found to be an extremal of the resulting trajectory flow to see if this satisfies the extremal condition for a distribution constrained by probability at a given epoch t, Eq. (67):

$$\Phi^T\Phi\delta\mathbf{x}_o = \sigma^2\Lambda_o\delta\mathbf{x}_o \tag{70}$$

$$\Phi^T\delta\mathbf{x} = \sigma^2\Lambda_o\delta\mathbf{x}_o \tag{71}$$

$$\delta\mathbf{x} = \sigma^2 \Phi^{-T} \Lambda_o \delta\mathbf{x}_o \tag{72}$$

$$\delta\mathbf{x} = \sigma^2 \Phi^{-T} \Lambda_o \Phi^{-1} \delta\mathbf{x} \tag{73}$$

But, by definition, $\Phi^{-T}\Lambda_o\Phi^{-1} = \Lambda(t, t_o)$, and we get

$$\delta\mathbf{x} = \sigma^2 \Lambda(t, t_o) \delta\mathbf{x} \tag{74}$$

equivalent to Eq. (67). We can note here that the eigenvalues of Λ_o do not map into the eigenvalues of $\Lambda(t)$, meaning that the direction of maximum elongation maps, in the future and in the past, into some other general direction on the ellipsoid surface.

The above discussion is in the context of extremal values of the state, which include maximum, minimum, and all intermediate axes on the ellipsoid. Evaluating the eigenvalues and eigenvectors of the covariance matrix immediately provides the values and directions of all these extreme values, where we note that the eigenvectors are all mutually orthogonal since the covariance matrix is symmetric in general. If the linear system is time invariant (motion about an equilibrium point) or corresponds to a time-periodic system (motion about a periodic orbit), then the limiting uncertainty directions can be defined as time grows large, and are identified as the unstable manifolds of the object. In this case, there is a correspondence between the limiting direction of uncertainty distribution and the eigenvectors and eigenvalues of the state transition matrix Φ [11]. For a general trajectory not associated with a specific geometric object in phase space, the limiting direction of uncertainty is not well defined over finite periods of time. Even though the characteristic exponent of the system is defined as $t \to \infty$, the evolution of this direction over time periods shorter than this may exhibit any number of transient phenomena. Situations of interest here, that have yet to be studied, include orbit-uncertainty distributions along quasi-periodic orbits (the Lissajous trajectories in the restricted three-body problem) and distributions along stable and unstable manifolds (such as the Genesis transfer trajectory towards and away from the halo orbit).

The implication of these results for orbit-uncertainty distributions relates to the probability of finding a spacecraft within some region of phase space projected into the measurement space in which the spacecraft is sensed and tracked. As the direction of uncertainty becomes pulled along the unstable manifolds of an orbit, the projected area in position and velocity space where the spacecraft can be found can become large, even though the total volume of the phase distribution is constant. Additionally, as certain regions of the probability distribution evolve far away from the nominal orbit, the effect of nonlinearities on the orbit distribution can begin to become important.

2. Uncertainty Distribution. A second issue beyond the direction in which the extremals of the distribution are arranged concerns the characterization of the distribution itself. For an ideal Hamiltonian system, the total volume of the constant probability distribution remains constant (by Liouville's theorem), meaning that the product of the eigenvalues of the covariance matrix $P(t, t_o)$, $\sigma_i^2; i = 1, 2, \cdots, 6$ is a constant, or that $\Pi_{i=1}^{6} \sigma_i(t)$ is a constant of the distribution. Furthermore, for a Hamiltonian system where the coordinates and momenta are properly distinguished (as can be done for any space trajectory problem), we also have constraints on the lower-order distributions of the phase flow via the integral invariants of the system. The implications of these powerful results of Hamiltonian systems for the statistical distribution of phase flow trajectories have yet to be analyzed in detail.

In [12], many of the above issues are discussed for the problem of describing uncertainty distributions in phase space. A number of specific results were derived that provide geometric descriptions of the evolution of a phase-space distribution. Although many options were considered, two main approaches emerged. The more general approach is to characterize the orbit distribution in terms of symplectic geometry, for which we have a number of very general and strong results, such as Liouville's theorem and the theory of

integral invariants. Additional mathematical progress must still be made in terms of the interpretation and application of these ideas to the distribution of orbit uncertainty. A simpler approach considers the geometry of position and velocity distributions independent of each other and develops simplified geometrical descriptors to give the current shape, size, and orientation of the uncertainty distribution.

Consider the three-dimensional uncertainty distribution of a spacecraft position. As described above, at each moment in time the distribution corresponds to an ellipsoid with distinct semimajor axes (related to the eigenvalues of the covariance matrix) that evolve in their size and orientation. The general shape characteristics of the distribution can be evaluated in terms of an index related to the geometric, arithmetic, and harmonic means of the semimajor axes. In particular, we can define a characteristic S:

$$S = \frac{HA}{G^2} \tag{75}$$

$$H = \frac{N}{\sum_{i=1}^{N} \frac{1}{a_i}} \text{ harmonic mean} \tag{76}$$

$$G = \left(\Pi_{i=1}^{N} a_i\right)^{1/N} \text{ geometric mean} \tag{77}$$

$$A = \frac{1}{N} \sum_{i=1}^{N} a_i \text{ arithmetic mean} \tag{78}$$

We note that the means satisfy the inequalities $H \leq G \leq A$, and hence $H/G \leq 1$ and $A/G \geq 1$. The combination of these two quantities in S indicates a direct measure of the shape of the distribution. If $N = 3$, we have $S = 1$ for a spherical distribution, $S < 1$ for a distribution compressed in one direction, and $S > 1$ for a distribution drawn out in one direction. The geometry of uncertainty distributions in unstable orbital environments was discussed and evaluated in [12] and can be directly related to the value of the S parameter discussed here.

3. Application to a 1-DOF Unstable System. Now, let us treat our simplified problem using the general analysis outlined above. First we note that, since our system is time invariant, we have an unstable manifold defined for $t \to \infty$, found by analyzing the eigenvalues and eigenvectors of the matrix Φ:

$$\sigma = \pm \lambda \tag{79}$$

$$\mathbf{u} = \frac{1}{\sqrt{1+\lambda^2}} \begin{bmatrix} 1 \\ \pm\lambda \end{bmatrix} \tag{80}$$

Realizing that the eigenvalue λ can be interpreted as the tangent of an angle γ_m, defining the direction of the stable and unstable manifold in phase space, we rewrite these as

$$\lambda = \pm \tan\gamma_m \tag{81}$$

$$\mathbf{u} = \begin{bmatrix} \cos\gamma_m \\ \pm \sin\gamma_m \end{bmatrix} \tag{82}$$

Now, let us consider the separate issues of the direction of the maximal distribution and the initial condition direction for the maximum distribution. In each case, we will consider an initial distribution $P_o = \Lambda_o = I$ for simplicity. Then the maximal distribution direction at a given time t is found as the maximum eigenvalue and corresponding eigenvector of the equation:

$$\left[\Phi(t,t_o)\Phi^T(t,t_o) - \sigma^2 I\right]\mathbf{u} = 0 \tag{83}$$

and the initial condition that gives the maximal distribution at a given time t is found as the maximum eigenvalue and corresponding eigenvector of the equation:

$$\left[\Phi^T(t,t_o)\Phi(t,t_o) - \sigma^2 I\right]\mathbf{u}_o = 0 \tag{84}$$

We note that these equations will have the same characteristic equation, as can be inferred given the correspondence between the eigenvectors: $\mathbf{u} = \Phi(t,t_o)\mathbf{u}_o$. For our simple case, this results in a characteristic equation:

$$0 = \sigma^4 - 2\sigma^2\left[1 + \frac{1}{2}\sinh^2(\lambda t)\left(\lambda + \frac{1}{\lambda}\right)^2\right] + 1 \tag{85}$$

$$\sigma_\pm^2 = 1 + \frac{1}{2}\sinh^2(\lambda t)\left(\lambda + \frac{1}{\lambda}\right)^2 \pm \sinh(\lambda t)\left(\lambda + \frac{1}{\lambda}\right)\sqrt{1 + \frac{1}{4}\sinh^2(\lambda t)\left(\lambda + \frac{1}{\lambda}\right)^2} \tag{86}$$

$$\sigma_+^2\sigma_-^2 = 1 \tag{87}$$

The direction of the maximum uncertainty in phase space at a given time is controlled by the eigenvector of Eq. (83) and is defined by the angle γ_P:

$$\tan\gamma_P = \frac{1}{2}\tanh(\lambda t)\left(\lambda - \frac{1}{\lambda}\right) + \sqrt{1 + \frac{1}{4}\tanh^2(\lambda t)\left(\lambda - \frac{1}{\lambda}\right)^2} \tag{88}$$

$$\tan(2\gamma_P) = \frac{1}{\tanh(\lambda t)}\tan(2\gamma_m) \tag{89}$$

$$\gamma_P = \frac{n\pi}{2} + \frac{1}{2}\arctan\left[\frac{\tan(2\gamma_m)}{\tanh(\lambda t)}\right] \tag{90}$$

where n even corresponds to $\sigma_+ > 1$ and n odd to $\sigma_- < 1$. Thus, as expected, we see that as $t \to \infty$, $\tanh(\lambda t) \to 1$, and $\gamma_P \to \gamma_m$. Conversely, if $t \to 0$, $\tan\gamma_P \to 1$, or $\gamma_P \to \pi/4$ initially. At $t = 0$, we actually have all directions having equivalent length, given our assumed identity initial covariance and information matrix. In general, we have the direction for the maximal distribution:

$$\mathbf{u} = \begin{bmatrix}\cos\gamma_P \\ \sin\gamma_P\end{bmatrix} \tag{91}$$

To find the initial condition that yields this maximal distribution, we can solve for the eigenvector of Eq. (84) or compute $\mathbf{u}_o = \Phi^{-1}(t, t_o)\mathbf{u} = \Phi(-t)\mathbf{u}$, which would be simpler for this system, yielding

$$\tan\gamma_{P_o} = \tan\gamma_m \frac{\tan\gamma_P - \tanh(\lambda t)\tan\gamma_m}{\tan\gamma_P \tanh(\lambda t) - \tan\gamma_m} \tag{92}$$

which can be reduced to

$$\tan 2\gamma_{P_o} = \frac{1}{\tanh(\lambda t)} \tan(\pi - 2\gamma_m) \tag{93}$$

$$\gamma_{P_o} = \frac{n\pi}{2} + \frac{1}{2}\arctan\left[\frac{\tan(\pi - 2\gamma_m)}{\tanh(\lambda t)}\right] \tag{94}$$

with the same rules for n even and odd, again. Now as $\lambda t \to \infty$, we see that $\gamma_{P_o} \to \pi/2 - \gamma_m$.

Thus, the optimal initial condition to fall under the influence of the unstable manifold does not lie on the unstable manifold but is shifted off of it. This can be understood when one considers the optimal initial condition to minimize the long-term state magnitude. This direction is orthogonal to the above direction, and thus is equal to $-\gamma_m$, which does lie on the stable manifold. That this minimizing direction must lie on the stable manifold can be understood in that any deviation from the stable manifold will carry the trajectory onto the unstable manifold and will increase its length. Next, we note that the extrema of the state are eigenvectors of the matrix $\Phi^T\Phi$, which is symmetric and which thus implies that all eigenvectors will be mutually orthogonal. Thus, since the stable and unstable manifolds are not mutually orthogonal in general, but are separated by an angle $2\gamma_m$, the optimal initial condition to increase the state cannot lie on the unstable manifold.

The orbit distribution parameters for our simple case are not as interesting, due to its low dimensionality. The more general case is discussed in [12]. For our 1-D case, the geometric mean $G = 1$, and the harmonic and arithmetic means are reciprocal, meaning that they measure $S = 1$ identically. Indeed, we find that

$$A = \frac{1}{2}\left[\sigma_+ + \frac{1}{\sigma_+}\right] \tag{95}$$

$$= \frac{1}{H} \tag{96}$$

As expected, we see that both A and $H \to \infty$ as $\lambda t \to \infty$, providing a measure of the elongation of the distribution.

B. Optimal Measurement Strategies

In [11], it was established that orbit-determination sensitivity can be related to the distribution of the orbit uncertainty, and hence to the unstable manifolds of an orbit. Thus, we can conceive of taking orbit-determination measurements at optimal times that will maximally increase the information content of the orbit (i.e., decrease covariance) and of avoiding measurements during times when we expect the increase in information content to be small.

1. Characterizing Measurements in Phase Space. As the spacecraft moves along its trajectory, it is occasionally tracked from an Earth station. In the following, we assume that the tracking stations

take Doppler data during each track. As is well known [7], the estimate that can be extracted from a pass of Doppler data is the spacecraft unit position vector and its line-of-sight velocity. Thus, in phase space, a pass of Doppler data is approximated by the measurements

$$\mathbf{h}_r = \hat{\mathbf{r}} \tag{97}$$

$$h_v = \hat{\mathbf{r}} \cdot \mathbf{v} \tag{98}$$

where $\hat{\mathbf{r}}$ is the unit position vector of the spacecraft and $\mathbf{v}$ is its velocity vector.

For our current analysis, we are interested in the information content of these measurements with respect to the state. This is computed by taking the partials of the measurements with respect to $\mathbf{r}$ and with respect to $\mathbf{v}$:

$$\frac{\partial \mathbf{h}_r}{\partial \mathbf{r}} = \frac{1}{r}\mathbf{U}_{rr} \tag{99}$$

$$\frac{\partial \mathbf{h}_r}{\partial \mathbf{v}} = 0 \tag{100}$$

$$\frac{\partial h_v}{\partial \mathbf{r}} = \frac{\mathbf{v}}{r} \cdot \mathbf{U}_{rr} \tag{101}$$

$$\frac{\partial h_v}{\partial \mathbf{v}} = \hat{\mathbf{r}} \tag{102}$$

$$\mathbf{U}_{rr} = [I - \hat{\mathbf{r}}\hat{\mathbf{r}}] \tag{103}$$

where $\mathbf{U}_{rr}$ is a dyad operator that removes the vector component parallel to the unit vector $\hat{\mathbf{r}}$. Thus, $\hat{\mathbf{r}} \cdot \mathbf{U}_{rr} = 0$, and if $\hat{\mathbf{r}}_\perp \cdot \hat{\mathbf{r}} = 0$, then $\hat{\mathbf{r}}_\perp \cdot \mathbf{U}_{rr} = \hat{\mathbf{r}}_\perp$.

Thus, in terms of the position component, the measurement $\mathbf{h}_r$ has a null space for orbit-uncertainty distributions along $\hat{\mathbf{r}}$, meaning that it cannot directly detect this component of an uncertainty distribution. The line-of-sight velocity measurement has its null space along this same direction, $\hat{\mathbf{r}}$, and also has a null space along the direction defined by $\hat{\mathbf{r}} \times \mathbf{v}$, and thus has a two-dimensional space where orbit-uncertainty distributions can "hide." For the velocity component of the partial, the $h_\mathbf{r}$ measurement has no information content, and the $h_\mathbf{v}$ measurement has a null space orthogonal to $\hat{\mathbf{r}}$.

When we combine these realizations with our realization that our orbit distribution will have a characteristic direction for maximum and minimum uncertainty, we see that there may be phase-space geometries at which a measurement can have an optimal impact on the uncertainty distribution (when it falls into the sensed direction) and other geometries where measurements prove to be ineffective (when it lies in the null space of $\partial h/\partial \mathbf{x}$). This issue has been studied for a spacecraft in an Earth–Sun halo orbit, tracked from the Earth, where it was found that the orientation of uncertainty was controlled to some extent by both the local unstable dynamics and by the phase-space geometry [11]. Specifically, in the absence of tracking, the orbit-uncertainty distribution is entrained along the unstable manifold of the orbit, as expected from our previous analysis. However, in the presence of measurements, the unstable manifolds become better determined, due to the sensitivity of errors in this direction. The axis of maximum uncertainty for these cases was oriented perpendicular to the local unstable manifold, in general, indicating

that these directions were preferentially determined. When the phase-space geometry was aligned so that the unstable manifold fell into the unobservable direction of the measurements, however, we saw that this situation was reversed and the direction of maximum uncertainty and the local unstable manifold became aligned again.

This indicates that a systematic approach to choosing optimal measurement times may be available, based on the local dynamics of the trajectory. In particular, if there exist certain periods of time when a fortuitous alignment between the sensing geometry and the distribution direction exists, we would expect a commensurate increase in our ability to determine the orbit with a single measurement. Should periods of poor alignment exist, we may defer measurement or schedule an increased number of measurements if this were to occur during a crucial period of the mission. This is, indeed, entirely analogous to the zero-declination singularity in Doppler tracking, but instead of arising purely from geometry, it arises due to the local dynamics along the spacecraft trajectory.

2. Application to a Simple 1-DOF Unstable System. To illustrate this, consider our basic 1-DOF system introduced earlier. Consider that we have an epoch information matrix of unity, $\Lambda_o = I$, and that we process a single measurement taken a time T after epoch, and represented as

$$h = \cos\gamma r + \sin\gamma v \tag{104}$$

where γ is a measurement parameter describing the direction, in phase space, that our measurement falls along. The question is, what is the optimal measurement geometry at a given epoch? The information content of the measurement can be computed to be

$$\delta\Lambda = \Phi^T(T)\frac{\partial h}{\partial x}\frac{\partial h}{\partial x}^T\Phi(T) \tag{105}$$

$$\frac{\partial h}{\partial x} = \begin{bmatrix}\cos\gamma \\ \sin\gamma\end{bmatrix} \tag{106}$$

To maximize the information content from a single measurement is equivalent to maximizing the determinant of $\Lambda_o + \delta\Lambda$, which leads to

$$|\Lambda_o + \delta\Lambda| = 1 + \cosh^2(\lambda T) + \sinh^2(\lambda T)\left[\lambda^2\sin^2\gamma + \frac{1}{\lambda^2}\cos^2\gamma\right]$$

$$+ 2\sinh(\lambda T)\cosh(\lambda T)\left(\lambda + \frac{1}{\lambda}\right)\sin\gamma\cos\gamma \tag{107}$$

To maximize this, we take the partial with respect to γ and equate the resultant to zero, finding

$$\sin 2\gamma\sinh^2(\lambda T)\left(\lambda + \frac{1}{\lambda}\right)\left(\lambda - \frac{1}{\lambda}\right) + 2\cos 2\gamma\sinh(\lambda T)\cosh(\lambda T)\left(\lambda + \frac{1}{\lambda}\right) = 0 \tag{108}$$

which can be solved for

$$\tan 2\gamma = \frac{2\lambda}{1-\lambda^2}\,\frac{1}{\tanh(\lambda T)} \tag{109}$$

Now note that we can interpret the parameter λ as the slope of the trajectory in phase space, or $\lambda = \tan\gamma_m$, where γ_m denotes the asymptotic direction of the hyperbolic motion in phase space, yielding

$$\tan 2\gamma = \frac{\tan 2\gamma_m}{\tanh(\lambda T)} \tag{110}$$

$$\gamma = \frac{n\pi}{2} + \frac{1}{2}\arctan\left[\frac{\tan 2\gamma_m}{\tanh(\lambda T)}\right] \tag{111}$$

Thus, for $T \ll 1$, the optimal measurement is taken along $\gamma \sim \pi/4$, and, as $T \gg 1$, the optimal measurement is taken along $\gamma \sim \gamma_m$, which is just the direction of the unstable manifold in phase space. A measurement along $\pi/2 + \gamma_m$, however, increases the information content by a minimum amount, decreasing to a zero change in information content if the time $\lambda t \to \infty$.

To generalize this result, we must acknowledge a number of constraints on our system. First, we do not have direct control over the measurement geometry, i.e., we cannot choose γ freely. But then, for a given γ, we can note when the optimal measurement geometry occurs and concentrate our efforts at that epoch. Similarly, the geometry and mechanics of determining optimal measurement epochs for a full 3-DOF system can become quite complicated. But in these situations, we can use the principle that optimal measurement geometries will occur when the measurement geometry in phase space is aligned with the unstable manifold geometry. Conversely, we may expect measurements at epochs when these directions are orthogonal to be not as effective.

C. Control of Unstable Trajectories

The mathematical instability of halo orbits has frequently discouraged missions from using halo orbits. This is unfortunate because the instability of halo orbits is a positive characteristic that enables very small and infrequent maneuvers in the absence of navigation errors (5 cm/s/year, 4 maneuvers/year). See [2,3] for a description of the pioneering work on the control of unstable trajectories for International Sun Earth Explorer 3 (ISEE3). Compared to low-altitude orbits with atmospheric drag, halo orbits are much easier to operate and maintain. Station keeping of halo orbits is one instance when navigation and trajectory design are tightly coupled. When orbital errors do build up, it typically is more expensive to correct to a nominal trajectory than to correct to a nearby halo orbit. But the nearby halo orbit must be designed to compensate for the errors as well as to fulfill the mission requirements and constraints. Due to the infrequency of halo orbit maneuvers for the Earth–Sun case, navigation teams have been able to iterate this labor-intensive process between the maneuver analysts and the trajectory designers to accomplish the error correction. One of the goals of an integrated nonlinear navigation and trajectory design approach is to streamline and eventually automate this process. Nonlinear dynamics hold the key to this problem because it provides a systematic approach to solving the nonlinear targeting problem for maintaining halo orbits.

1. Nonlinear Control. Recent developments using dynamical systems theory have opened new possibilities for the control and design of halo orbit missions [5]. See [9] and [10] for some new applications based on these approaches. In [5], a station-keeping algorithm using invariant manifold theory is developed. The basic idea is to decompose the linear approximation to the state space into the form $S \times U \times C$, where S is the stable subspace, U is the unstable subspace, and C is the center subspace, each approximating an invariant manifold of the same name. By watching the growth of the U-component and killing it with a maneuver when it gets too large, a simple control algorithm to maintain the halo orbit is achieved that may be automated. The actual algorithm requires a more careful analysis of the center manifold, where secular drifts may occur, but this is well-known and there are algorithms to control this effectively. Howell and Pernicka [8] have developed a target-point method that was used for the analysis of the Genesis station-keeping maneuvers; see [13] for more details and references to the Genesis work.

This approach to control follows along more standard navigation practices, as it uses the linearized motion about a trajectory to arrive at their control. By combining these approaches to nonlinear control, an effective class of nonlinear station-keeping algorithms may be developed. In addition, the nonlinear navigation algorithm may be folded into the station-keeping algorithm to provide a more effective and robust control of the halo orbit. This will bring us one step closer to the full automation of the navigation and trajectory planning capability in unstable orbital environments.

2. Optimal Statistical Maneuver Placement. The fundamental metrics of navigation performance are the fuel expended in controlling the trajectory and the frequency of maneuvers needed to control the trajectory. As described previously, the statistical characterization of these costs can be defined for any general trajectory and probability distribution. Thus, a decrease in the cost of these maneuvers can be achieved in one of two ways: either reduce the overall uncertainty or choose the timings of the maneuvers to reduce the statistical cost. Reduction in uncertainty includes optimally tracking the spacecraft as well as reducing control errors (which are not explicitly discussed here). The issue of optimal tracking was already described. Thus, we can consider the optimal placement of maneuvers.

In general, we can use the mean ΔV to constrain the magnitude of the statistical maneuvers, allowing us to use the limit on $\overline{\Delta V}$ derived previously:

$$\overline{\Delta V} \leq \sqrt{2}\,\frac{\Gamma\left(\frac{N}{2}+\frac{1}{2}\right)}{\Gamma\left(\frac{N}{2}\right)}\|\Psi R^{-1}\|_2 \tag{112}$$

which means that to bound the mean of any statistical maneuver will require only that the eigenvalues of $R^{-T}\Psi^T\Psi R^{-1}$ be evaluated, the coefficient of the inequality being

$$\sqrt{2}\,\frac{\Gamma\left(\frac{N}{2}+\frac{1}{2}\right)}{\Gamma\left(\frac{N}{2}\right)} = \begin{cases} \dfrac{\sqrt{2\pi}(2n)!}{2^{2n}(n-1)!n!} & N=2n \\ \sqrt{\dfrac{2}{\pi}}\dfrac{2^{2n}(n!)^2}{(2n)!} & N=2n+1 \end{cases} \tag{113}$$

Thus, the bound involves the linear solution of motion about the trajectory and the uncertainty distribution at the initial epoch. Considering the uncertainty distribution to be controlled by the measurement sequence (discussed previously), the only remaining degree of freedom is to choose the maneuver times t_1 and t_2 to minimize the mean maneuver size. For a given trajectory, and a given set of generic initial uncertainties, this is a relatively simple computation to make for a single maneuver. Of more interest is the design of a sequence of such maneuvers to find the optimal maneuver frequency. If the spacecraft is being controlled about an equilibrium point, then the dynamics matrix Ψ will be invariant from maneuver to maneuver, and a general formula can be developed easily. For the control of a trajectory along a periodic orbit, or along a more general nonperiodic motion, the dynamics matrix will become a function of location along the orbit, leading to a more complicated analysis that relies on numerical solutions to a time-varying linear differential equation.

3. Application to a 1-DOF Unstable System. Again, for the analysis of an unstable system, we can turn to our simple 1-DOF motion. Recall that, in this case, we can choose the correction sequence as a maneuver after a time T from the previous control maneuver with the second maneuver designed to lie at $t_2 \to \infty$, at which time the controlled trajectory will asymptotically approach the origin. Naturally, this second maneuver is never performed, and the first maneuver is repeated after every time T. For our system, the cost of each maneuver, given a current position and velocity error of δr and δv, is

$$\Delta V = e^{\lambda T} \left| \lambda \delta r + \delta v \right| \tag{114}$$

which is calculated by combining Eqs. (46) and (47) with Eq. (61). Thus, the longer the maneuver is delayed, the larger it becomes. Carrying out the detailed integrations yields (assuming $\sigma_{rv} = 0$ initially)

$$\overline{\Delta V} = \sqrt{\frac{2}{\pi}} e^{\lambda T} \sqrt{\lambda^2 \sigma_r^2 + \sigma_v^2} \tag{115}$$

$$\sigma_{\Delta V}^2 = e^{2\lambda T} \left(1 - \frac{2}{\pi} \right) \left(\lambda^2 \sigma_r^2 + \sigma_v^2 \right) \tag{116}$$

giving us explicit formulae for the statistical cost of maneuvers.

Let us also develop the bound on the mean ΔV, independent of the probability integral outlined above. For this we need to properly identify the matrix $\Psi = e^{\lambda T}[\lambda, 1]$ and the inverse of the square-root information matrix, $R^{-1} = [\sigma_r, 0 : 0, \sigma_v]$. Combining these together yields $\Psi R^{-1} = e^{\lambda T}[\sigma_r \lambda, \sigma_v]$, which has a 2-norm $e^{\lambda T} \sqrt{\lambda^2 \sigma_r^2 + \sigma_v^2}$. Now note that $N = 2$ for our case, and thus that $\sqrt{2}\Gamma(3/2)/\Gamma(1) = \sqrt{\pi/2}$, yielding the inequality

$$\overline{\Delta V} \leq \sqrt{\frac{\pi}{2}} e^{\lambda T} \sqrt{\lambda^2 \sigma_r^2 + \sigma_v^2} \tag{117}$$

which reduces to the inequality $\sqrt{2/\pi} \leq \sqrt{\pi/2}$, which is always true.

We note immediately that the cost of maneuvers (both computed and bounded) always will be proportional to $e^{\lambda T}$. We can use this result to compute the optimal maneuver frequency along an unstable trajectory.

Assume we wish to control a trajectory over an extended period of time τ, and that we wish to perform a maneuver after every time T, resulting in a total of $M = \tau/T$ maneuvers. Then the total statistical cost of this sequence of maneuvers is

$$\Delta V_n = M e^{\lambda T} \sqrt{\frac{2}{\pi}} \left[1 + \frac{1}{\sqrt{M}} \sqrt{\frac{\pi}{2} - 1} \right] \sqrt{\lambda^2 \sigma_r^2 + \sigma_v^2} \tag{118}$$

$$\Delta V_n = \frac{\lambda \tau}{\lambda T} e^{\lambda T} \sqrt{\frac{2}{\pi}} \left[1 + \sqrt{\frac{\lambda T}{\lambda \tau}} \sqrt{\frac{\pi}{2} - 1} \right] \sqrt{\lambda^2 \sigma_r^2 + \sigma_v^2} \tag{119}$$

Thus, we see that the total cost is proportional to the term

$$\frac{e^x}{x} \left[1 + \sqrt{\frac{x}{\lambda \tau}} \sqrt{\frac{\pi}{2} - 1} \right] \tag{120}$$

where $x = \lambda T$ is the variable and $\lambda \tau$ is a free parameter. For simplicity, assume $\tau \to \infty$, meaning that the statistical cost of the maneuvers is controlled by the mean value of each maneuver, and yielding the simpler proportionality factor e^x/x. Taking the partial of this with respect to x, setting it equal to zero,

and solving for x yields the simple optimum $x = 1$, which then gives us our optimal maneuver frequency as

$$T = \frac{1}{\lambda} \tag{121}$$

or one maneuver after every characteristic time of the unstable system. This is significant because it directly links the local characterization of the trajectory to the appropriate control strategy. Figure 2 shows Eq. (120) for several values of $\lambda\tau$, showing that the optimum spacing does not vary much from $\lambda T = 1$.

This simple result can be used as a design principle in developing a control strategy for an unstable trajectory, using the local characteristic time of the trajectory as the nominal correction maneuver time. When applying this result to full 3-DOF systems targeted to time-varying trajectories, the resultant equations are not as simple. For example, it is not possible to place the trajectory directly onto the stable manifold for a 2-DOF or higher system, as the stable and unstable manifolds will occupy different locations in configuration space, unlike the 1-DOF problem, where these manifolds overlap in configuration space. Still, generalizations of this result to multiple-maneuver correction strategies still result in optimal maneuver spacings on the order of one characteristic time.

V. Future Directions

This article presents some basic ideas and facts associated with the statistical distribution of trajectories in orbit-determination problems. Several possible measures of navigation performance are developed based on geometric ideas and are related to a particular class of geometric shapes. These measures are then evaluated in a test case of spacecraft orbit determination in an unstable halo periodic orbit in the Earth–Sun system. We find that certain correlations exist between the measures and the dynamical environment found in the system. Future work will apply the methods outlined here to station keeping about an unstable equilibrium point and about an unstable halo orbit in the restricted three-body problem and in the Hill three-body problem.

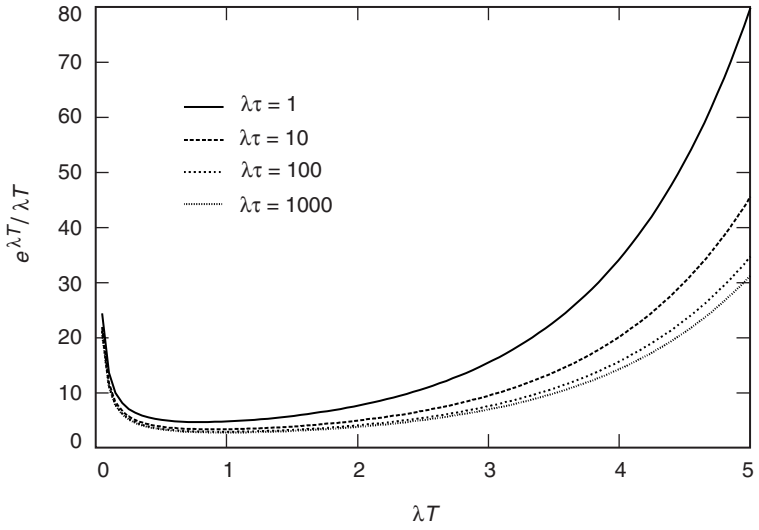

Fig. 2. Scaling factor for the statistical cost of station-keeping maneuvers as a function of frequency of station-keeping maneuvers for different values of total time $\lambda\tau$.

References

[1] G. J. Bierman, *Factorization Methods of Discrete Sequential Estimation*, San Diego, California: Academic Press, 1977.

[2] R. W. Farquhar, D. P. Muhonen, C. R. Newman, and H. S. Heuberger, "Trajectories and Orbital Maneuvers for the First Libration-Point Satellite," *Journal of Guidance and Control*, vol. 3, no. 6, pp. 549-554, November–December 1980.

[3] R. W. Farquhar, D. Muhonen, and L. Church, "Trajectories and Orbital Maneuvers for the ISEE-3/ICE Comet Mission," *Journal of the Astronautical Sciences*, vol. 33, pp. 235–254, July–September 1985.

[4] C. Froeschlé, "The Lyapunov Characteristic Exponents—Applications to Celestial Mechanics," *Celestial Mechanics*, vol. 34, pp. 95–115, 1984.

[5] G. Gomez, J. Llibre, R. Martinez, and C. Simo, "Dynamics and Mission Design Near Libration Points," *World Scientific Monograph Series in Mathematics*, vol. 2, pp. 45–58, 2001.

[6] D. T. Greenwood, *Classical Dynamics*, Mineola, New York: Dover, pp. 182–183, 1997.

[7] T. W. Hamilton and W. G. Melbourne, "Information Content of a Single Pass of Doppler Data from a Distant Spacecraft," *Space Programs Summary 37-39*, vol. III, Jet Propulsion Laboratory, Pasadena, California, pp. 18–23, March–April 1966.

[8] K. C. Howell and H. J. Pernicka, "Stationkeeping Method for Libration Point Trajectories," *Journal of Guidance and Control*, vol. 16, no. 1, pp. 151–159, 1993.

[9] K. C. Howell, B. T. Barden, R. S. Wilson, and M. W. Lo, "Trajectory Design Using a Dynamical Systems Approach with Application to Genesis," AAS paper 97-709, AAS/AIAA Astrodynamics Specialists Conference, Sun Valley, Idaho, August 4–7, 1997.

[10] M. Lo, B. Williams, W. Bollman, D. Han, Y. Hahn, J. Bell, E. Hirst, R. Corwin, P. Hong, K. Howell, B. Barden, and R. Wilson, "Genesis Mission Design," AIAA paper 98-4468, AIAA/AAS Astrodynamics Conference, Boston, Massachusetts, August 10–12, 1998.

[11] D. J. Scheeres, D. Han, and Y. Hou, "The Influence of Unstable Manifolds on Orbit Uncertainty," *Journal of Guidance, Control, and Dynamics*, vol. 24, no. 3, pp. 573–585, 2001.

[12] D. J. Scheeres, "Characterizing the Orbit Uncertainty Dynamics Along an Unstable Orbit," AAS paper 01-302, presented at the 2001 AAS/AIAA Astrodynamics Specialist Meeting, Quebec City, Canada, August 2001.

[13] K. Williams, B. T. Barden, K. C. Howell, R. S. Wilson, and M. W. Lo, "Genesis Halo Orbit Station Keeping Design," ISSFD Conference, Biarritz, France, June 2000.